Publications of the Astronomical Society of the Pacific, **122**:499–515, 2010 May

The Herschel ATLAS

S. Eales,[1] L. Dunne,[2] D. Clements,[3] A. Cooray,[4] G. De Zotti,[5] S. Dye,[1] R. Ivison,[6] M. Jarvis,[7] G. Lagache,[8] S. Maddox,[2] M. Negrello,[9] S. Serjeant,[9] M. A. Thompson,[7] E. Van Kampen,[10] A. Amblard,[4] P. Andreani,[10] M. Baes,[11] A. Beelen,[8] G. J. Bendo,[3] D. Benford,[12] F. Bertoldi,[13] J. Bock,[14] D. Bonfield,[7] A. Boselli,[15] C. Bridge,[16] V. Buat,[15] D. Burgarella,[15] R. Carlberg,[17] A. Cava,[18] P. Chanial,[3] S. Charlot,[19] N. Christopher,[20] P. Coles,[1] L. Cortese,[1] A. Dariush,[1] E. da Cunha,[21] G. Dalton,[22] L. Danese,[23] H. Dannerbauer,[24] S. Driver,[25] J. Dunlop,[26] L. Fan,[23] D. Farrah,[27] D. Frayer,[28] C. Frenk,[29] J. Geach,[29] J. Gardner,[12] H. Gomez,[1] J. González-Nuevo,[23] E. González-Solares,[30] M. Griffin,[1] M. Hardcastle,[7] E. Hatziminaoglou,[10] D. Herranz,[31] D. Hughes,[32] E. Ibar,[6] Woong-Seob Jeong,[33] C. Lacey,[29] A. Lapi,[34] A. Lawrence,[26] M. Lee,[35] L. Leeuw,[36] J. Liske,[10] M. López-Caniego,[37] T. Müller,[38] K. Nandra,[3] P. Panuzzo,[39] A. Papageorgiou,[1] G. Patanchon,[40] J. Peacock,[26] C. Pearson,[41] S. Phillipps,[42] M. Pohlen,[1] C. Popescu,[43] S. Rawlings,[20] E. Rigby,[2] M. Rigopoulou,[22] A. Robotham,[25] G. Rodighiero,[44] A. Sansom,[43] B. Schulz,[16] D. Scott,[45] D. J. B. Smith,[2] B. Sibthorpe,[6] I. Smail,[29] J. Stevens,[7] W. Sutherland,[46] T. Takeuchi,[47] J. Tedds,[48] P. Temi,[36] R. Tuffs,[49] M. Trichas,[3] M. Vaccari,[44] I. Valtchanov,[50] P. van der Werf,[51] A. Verma,[20] J. Vieria,[16] C. Vlahakis,[51] and Glenn J. White,[9,41]

Received 2009 October 19; accepted 2010 March 29; published 2010 April 22

ABSTRACT. The Herschel ATLAS is the largest open-time key project that will be carried out on the *Herschel Space Observatory*. It will survey 570 deg^2 of the extragalactic sky, 4 times larger than all the other Herschel extragalactic surveys combined, in five far-infrared and submillimeter bands. We describe the survey, the complementary multiwavelength data sets that will be combined with the Herschel data, and the six major science programs we are undertaking. Using new models based on a previous submillimeter survey of galaxies, we present predictions of the properties of the ATLAS sources in other wave bands.

Online material: color figures

1. INTRODUCTION

Approximately half the energy emitted since the big bang by all of the objects in the universe has been absorbed by dust and then reradiated between 60 and 500 μm (Dwek et al. 1998; Fixsen et al. 1998; Driver et al. 2008), a wavelength range in which the universe is still largely unexplored (Fig. 1). On the short-wavelength side of this wave band, the whole sky was surveyed at 60 and 100 μm by IRAS in the 1980s. However, almost all of the tens of thousands of galaxies detected by IRAS were

[1] School of Physics and Astronomy, Cardiff University, Queens Buildings, The Parade, Cardiff CF24 3AA, UK.

[2] School of Physics and Astronomy, University of Nottingham, Nottingham, NG7 2RD, UK.

[3] Physics Department, Imperial College London, Prince Consort Road, London, SW7 2AZ, UK.

[4] Center for Cosmology, University of California, Irvine, CA 92697.

[5] INAF-Osservatorio Astronomico di Padova, I-35122 Padova, and SISSA, I-34014 Trieste, Italy.

[6] UK Astronomy Technology Centre, Royal Observatory, Blackford Hill, Edinburgh EH9 3HJ, UK.

[7] Centre for Astrophysics Research, STRI, University of Hertfordshire, Hatfield, AL10 9AB, UK.

[8] Institut d'Astrophysique Spatiale (IAS), batiment 121, Université Paris-Sud 11 and CNRS (UMR 8617), 910405 Orsay, France.

[9] Dept. of Physics and Astronomy, The Open University, Milton Keynes, MK7 6AA, UK.

[10] European Southern Observatory, Karl-Schwarzschild-Str. 2, 85748 Garching bei München, Germany.

[11] Sterrenkundig Observatorium, Universiteit Gent, Krijgslaan 281 S9, B-9000 Gent, Belgium.

[12] Observational Cosmology Laboratory, NASA–Goddard Space Flight Center, Greenbelt MD 20771.

[13] Argelander Institute for Astronomy, Bonn University, Auf dem Huegel 71, D-53121 Bonn, Germany.

[14] Astrophysics and Space Science, Jet Propulsion Laboratory, Pasadena, CA, 91109 and Department of Physics, Math and Astronomy, California Institute of Technology, Pasadena, CA, 91125.

[15] Laboratoire d'Astrophysique de Marseille, OAMP, Université Aix-Marseille, CNRS, 38 Rue Frédéric Joliot-Curie, 13388 Marseille cedex 13, France.

[16] California Institute of Technology, Pasadena, CA 91125.

[17] Department of Astronomy and Astrophysics, 50 St. George Street, Toronto, Ontario, M5S 3H4, Canada.

[18] Instituto de Astrofisica de Canarias, C/ Via Lactea s/n, E-38200 La Laguna, Spain.

spirals and starbursts in the nearby universe ($z < 0.1$), and IRAS revealed little about the dust in other galaxy populations, especially early-type galaxies (Bregman et al. 1998). Even in the late-type galaxies, only the small fraction of the dust warm enough to radiate significantly in the far-infrared was detected by IRAS. Devereux & Young (1990), for example, showed that the gas-to-dust ratio estimated from IRAS measurements alone was $\simeq 10$ times greater than the standard Galactic value, implying that $\simeq 90\%$ of the dust in galaxies was effectively missed by IRAS. ISO and *Spitzer*, with their long wavelength (170 μm) band, suffered less from this problem but will still have effectively missed any dust with $T < 15$ K (Bendo et al. 2003). Notwithstanding the successes of IRAS, ISO, and *Spitzer*, most of the wave band from 60 to 500 μm is still virtually terra incognita, and the only survey of a large area of the extragalactic sky at a wavelength beyond 200 μm is the one recently carried out by the Herschel pathfinder experiment, the Balloon-borne Large-Aperture Submillimeter Telescope (BLAST), which covered $\simeq 20$ deg^2 at 250 μm, 350 μm, and 500 μm (Devlin et al. 2009).

The lack of a survey covering a large area of sky in the submillimeter wave band (in this article defined as 100 μm $< \lambda < 1$ mm) has left us in some ways knowing more about dust in the distant, early universe than in the universe today. The surveys that have been carried out in the submillimeter wave band with ground-based telescopes—at 450 μm and 850 μm with the SCUBA camera on the James Clerk Maxwell Telescope (Hughes et al. 1998; Eales et al. 1999; Coppin et al. 2006), at 1.2 mm with MAMBO on the IRAM 30 m telescope (Greve et al. 2004; Bertoldi et al. 2007; Greve et al. 2008) and at 1.1 mm with AzTEC on the James Clerk Maxwell Telescope (Perera et al. 2008; Scott et al. 2008)—have been of very small areas of sky, covering ~1 deg^2 of sky in total. Because of the unusual submillimeter "K-correction,"[52] these surveys have mostly detected sources at very high redshifts ($z \gtrsim 1$). They have led to the important discovery that there is a population of luminous dust-enshrouded galaxies in the early universe (Smail et al. 1997; Hughes et al. 1998), which many authors have suggested are the ancestors of ellipticals today (Scott et al. 2002; Dunne et al. 2003), but they have told us relatively little about the evolution of the universe since $z \simeq 1$ (the last 8 billion yr) and almost nothing at all about dusty galaxies in the nearby universe.

Two basic things one would like to know about the nearby universe are the submillimeter luminosity function and the

[19] Institut d'Astrophysique de Paris, CNRS UMR7095 UPMC, 98 bis boulevard Arago, F-75014 Paris, France.
[20] Oxford Astrophysics, Denys Wilkinson Building, University of Oxford, Keble Road, Oxford, OX1 3RH, UK.
[21] Department of Physics, University of Crete, 71003 Heraklion, Greece.
[22] Astrophysics, University of Oxford, Oxford OX1 3RH and The Rutherford Appleton Laboratory, Chilton, Didcot, OX11 0QX, UK.
[23] SISSA, Via Beirut 2-4, I-34014 Trieste, Italy.
[24] Max-Planck-Institute for Astronomy, Konigstuhl 17, D-69117 Heidelberg, Germany.
[25] School of Physics and Astronomy, University of St Andrews, St Andrews, KY16 9SS, UK.
[26] Institute for Astronomy, University of Edinburgh, Royal Observatory, Edinburgh EH9 3HJ, UK.
[27] Astronomy Centre, University of Sussex, Brighton, UK.
[28] Infrared Processing and Analysis Center, California Institute of Technology, Pasadena, CA 91125.
[29] Institute for Computational Cosmology, Physics Dept., Durham University, South Road, Durham DH1 3LE, UK.
[30] Institute of Astronomy, University of Cambridge, Madingley Rd., Cambridge CB3 0HA, UK.
[31] Instituto de Física de Cantabria (CSIC-UC), Santander 39005, Spain.
[32] Instituto Nacional de Astrofísica, Optica y Electrónica (INAOE), Aptdo. Postal 51 y 216, Puebla, Mexico.
[33] Space Science Division, Korea Astronomy & Space Science Institute, 61-1, Hwaam-dong, Yuseong-gu, Daejeon, 305-348, Republic of Korea.
[34] Physics Dept., University Tor Vergata, Via della Ricerca Scientifica 1, I-00133 Rome, Italy.
[35] Astronomy Program, Department of Physics and Astronomy, Seoul National University, Seoul 151-742, Korea.
[36] Astrophysics Branch, NASA Ames Research Center, Moffett Field, CA 94035.
[37] Instituto de Física de Cantabria (CSIC-UC), Santander, 39005, Spain.
[38] Max-Planck-Institut für extraterrestrische Physik, Giessenbachstr., 85748 Garching, Germany.
[39] CEA, Laboratoire AIM, Irfu/SAp, F-91191 Gif-sur-Yvette, France.
[40] Université Denis Diderot, Laboratoire Astro-Particules et Cosmologie, 10 rue Alice Domon et Léonie Duquet, 75205, Paris Cedex 13, France.
[41] Rutherford Appleton Laboratory, Chilton, Didcot, Oxfordshire OX11 0QX, UK.
[42] Astrophysics Group, Department of Physics, University of Bristol, Tyndall Avenue, Bristol BS8 1TL, UK.
[43] Jeremiah Horrocks Institute, University of Central Lancashire, Preston, PR1 2HE, UK.
[44] Department of Astronomy, University of Padova, Vicolo Osservatorio 3, I-35122, Padova, Italy.
[45] Department of Physics & Astronomy, University of British Columbia, 6224 Agricultural Road, Vancouver BC, V6T1Z1, Canada.
[46] Astronomy Unit, Queen Mary University of London, Mile End Road, London E1 4NS, UK.
[47] Institute for Advanced Research, Nagoya University, Furo-cho, Chikusa-ku, Nagoya 464-8601, Japan.
[48] Department of Physics and Astronomy, University of Leicester, University Road, Leicester LE1 7RH, UK.
[49] Max-Planck-Institut für Kernphysik, Saupfercheckweg 1, D-69117, Heidelberg, Germany.
[50] Herschel Science Centre, ESA, P.O. Box 78, 28691 Villanueva de la Caada, Madrid, Spain.
[51] Leiden Observatory, Leiden University, P.O. Box 9513, NL-2300 RA Leiden, The Netherlands.

[52] Beyond a redshift of $\simeq 1$, as the redshift of a dusty galaxy increases, its characteristic spectral energy distribution ensures that the effect of the increasing luminosity-distance on its observed flux density is balanced by the increasing rest-frame luminosity of the galaxy. The consequence is that the galaxy's flux density is approximately independent of redshift.

[53] This forms about $2/3$ of the total observing time on Herschel, with the remaining $1/3$ being time reserved for the teams that built the instruments —"Guaranteed Time."

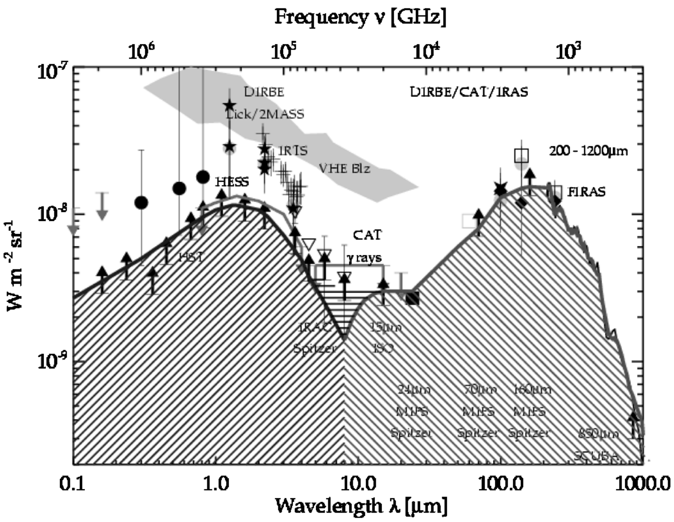

FIG. 1.—Extraglactic background radiation as a function of wavelength (Dole et al. 2006). See the electronic edition of the PASP for a color version of this figure.

dust-mass function: the space-density of galaxies as a function of luminosity and dust mass, respectively. These functions are important for many reasons, including tests of semianalytical models of galaxy formation (Cole et al. 2000; Baugh et al. 2005) and, by comparison with the same functions at high redshift, accurate measurements of the amount of evolution that is occurring in the submillimeter wave band (Dunne et al. 2003). Unfortunately, our knowledge of these functions is still extremely poor because of the limitations in areal coverage and sensitivity of previous submillimeter telescopes. Until recently, the only estimates of the local submillimeter luminosity function were one based on 55 galaxies detected in an ISO 170 μm survey (Takeuchi et al. 2006) and one based on SCUBA 850 μm observations of $\simeq$200 galaxies selected in other wave bands (Dunne et al. 2000; Vlahakis et al. 2005). There are now direct estimates from the BLAST results of the local luminosity function at 250 μm, 350 μm, and 500 μm (Eales et al. 2009), but their accuracy is limited by the small number of low-redshift sources detected in the BLAST survey: $\simeq$30 at $z < 0.2$.

The lack of a large-area survey capable of measuring the dust content and dust-obscured star formation in large numbers of galaxies in the local universe has been especially galling for submillimeter astronomers in the light of the success of their colleagues working in other wave bands. The Sloan Digital Sky Survey (SDSS) and the Two Degree Field Galaxy Redshift Survey (2dFGRS) have led to a revolution in our understanding of the distribution of galaxies in the local universe and the relationships between their present star-formation rate, star-formation history, stellar mass, morphology, and environment (Lewis et al. 2002; Kauffmann et al. 2003a, 2003b; Heavens et al. 2004; Balogh et al. 2004). However, all of the studies that have used these impressive data sets to investigate the physics and ecology of the galaxy population have been forced to ignore the dust phase of the interstellar medium and star formation that is heavily obscured by dust. The sensitivity of the IRAS survey was only sufficient to detect a small percentage of the galaxies in the redshift surveys (1.8% of the SDSS galaxies–Obric et al. 2006), and IRAS missed 90% of the dust in the detected galaxies because of its insensitivity to cold dust (Devereux & Young 1990).

The launch of the *Herschel Space Observatory*, which occurred on 2009 May 14, has the potential to dramatically increase our knowledge of dust and dust-obscured star formation, especially in the nearby universe. *Herschel* has two main cameras: SPIRE, which is able to image the sky simultaneously at 250 μm, 350 μm, and 500 μm (Griffin et al. 2007), and PACS, which is able to image the sky in two bands simultaneously, either 70 μm and 170 μm or 110 μm and 170 μm (Poglitsch et al. 2006). *Herschel* has much better angular resolution ($\simeq 18''$ at 250 μm) and sensitivity than previous observatories, and the spectral coverage of SPIRE will make it possible to carry out the first large-area surveys in this virtually unexplored part of the electromagnetic spectrum. The SPIRE bands will also make it possible to detect the cold dust that was missed by earlier observatories. *Herschel* is also better suited for investigating the local universe than the submillimeter surveys that will soon be carried out from the ground, in particular the SCUBA-2 and LABOCA surveys, because these will mostly be 850 μm, where low-redshift galaxies are intrinsically faint, whereas the *Herschel* bands span the peak of the typical spectral energy distribution of a galaxy in the nearby universe.

In this article, we describe the largest project that will be carried out with the *Herschel Space Observatory* in open time, the time available for competition within the international astronomical community.[53] The Herschel Astrophysical Terahertz Large Area Survey (the Herschel ATLAS or H-ATLAS) will be a survey of 570 $\deg^2$ of sky in five photometric bands. This is $\simeq$8 times larger than the coverage of the next largest (in area) Herschel extragalactic survey, HERMES (Oliver et al. 2010). The main scientific goal of the H-ATLAS is to provide measurements of the dust masses and dust-obscured star formation for tens of thousands of nearby galaxies, the far-IR/submillimeter equivalent to the SDSS photometric survey. However, the H-ATLAS has many other science goals ranging from the investigation of the point sources that will be detected by the Planck Surveyor to a study of high-latitude galactic dust.

The arrangement of this article is as follows. In § 2 we describe the basic parameters of the survey. In § 3 we present predictions of the number and redshift distribution of the sources that will be detected by the H-ATLAS. In § 4, we describe the complementary data that exists or will soon exist for the H-ATLAS fields. In § 5 we describe the six main H-ATLAS science programs. In § 6 we describe the detailed survey strategy, including issues that will be of interest to the general community, such as our plans for the release of data products. We everywhere assume the cosmological parameters for a "concordance universe": $\Omega_M = 0.267$ and $\Omega_\Lambda = 0.732$.

2. THE BASIC PARAMETERS OF THE SURVEY

The H-ATLAS has been allocated 600 hr of time, making it the largest key project that will be carried out with *Herschel* in open time. For all of our science goals (§ 5), the final sensitivity of the survey is not critical, and it is more important to survey the greatest possible area of sky. We have therefore chosen to use the maximum possible scan rate for the telescope ($60'' \, s^{-1}$). For our first science program (§ 5.1), it is important to make observations with PACS and SPIRE, and therefore we have chosen to use the *Herschel* observing mode that allows simultaneous observations with the two cameras: Parallel Mode (PMode). Of the two possible combinations of photometric bands for PACS (Poglitsch et al. 2006), we have chosen to observe at 110 μm and 170 μm rather than at 70 μm and 170 μm, mostly on the grounds of sensitivity; the noise at 70 μm and 110 μm should be fairly similar but galaxies, even at low redshift, are generally brighter at the longer wavelength. Although this combination will be worse for estimating the temperature of the dust, our models suggest that we will still be able to obtain useful measurements of the temperature of the dust in low-redshift galaxies.

With an eye on the legacy value of the H-ATLAS, we have chosen to observe fields in the northern and southern hemispheres and on the celestial equator. Other than that, we have chosen our fields to maximise the amount of complementary data and to minimize the amount of confusing emission from dust in the Galaxy, this last determined from the IRAS 100 μm maps. The fields, which are shown in Figure 2 and listed in Table 1, are:

1. One field close to the north Galactic pole with an area of $150 \ \deg^2$ (henceforth the NGP field);

2. Three fields, each of approximately $56 \ \deg^2$ in area, coinciding with the fields being surveyed in the Galaxy And Mass Assembly redshift survey (Driver et al. 2009) (henceforth the GAMA fields);

3. Two fields with a total area of $250 \ \deg^2$ close to the south Galactic pole (henceforth the SGP fields).

The total survey covers $570 \ \deg^2$. The angular resolution (full width at half-maximum, FWHM) of the observations will be approximately 8″, 12″, 18″, 25″, and 36″ at 70 μm, 110 μm, 250 μm, 350 μm, and 500 μm, respectively. We used the *Herschel* observation planning package HSpot to estimate the sensitivities we should reach in the five bands, on the assumption that the sources will be unresolved by the telescope beam and neglecting the effects of the emission from dust in the Galaxy and of confusion from extragalactic sources. With these assumptions, our prelaunch predictions for the 5σ sensitivities that should be reached in the five bands were 67 mJy at 110 μm, 94 mJy at 170 μm, 45 mJy at 250 μm, 62 mJy at 350 μm, and 53 mJy at 500 μm. At the time of writing, our analysis of the first H-ATLAS observations has shown that we are actually doing better than this in the SPIRE bands but not quite as well in the PACS bands. As the data-reduction pipelines are still under development, and so the current sensitivity estimates are not yet final, in the modeling described in the next section we have used the predicted sensitivities rather than the current measured sensitivities.

3. PREDICTIONS

The number of sources that will be found in any of the Herschel surveys is uncertain because they cover regimes of flux density and wavelength that have never been explored before. There is a particular problem in the wavelength range $200 < \lambda < 500$ μm because no survey, until the very recent survey with the balloon-borne telescope BLAST (Devlin et al. 2009), has been carried out at these wavelengths. Models based on

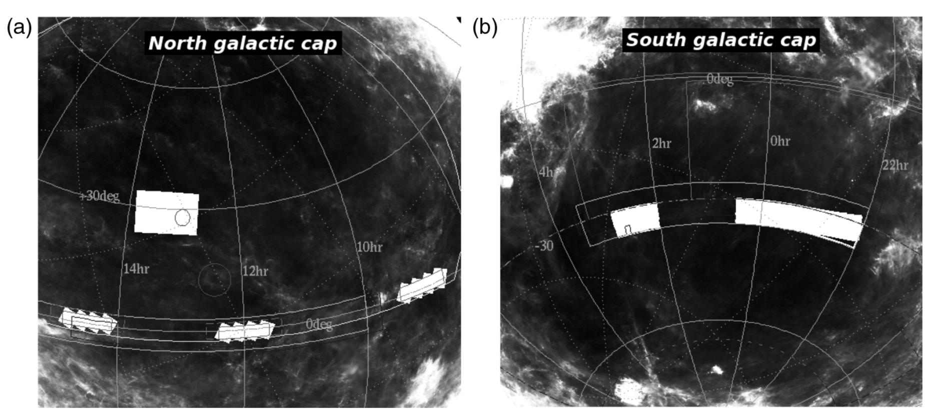

FIG. 2.—Positions of the ATLAS fields, shown as white blocks, superimposed on the IRAS 100 μm map of the sky, which traces the distribution of galactic dust. *Left* the northern galactic cap, *right* the southern galactic cap. See the electronic edition of the PASP for a color version of this figure, which shows the coverage of the complementary multiwavelength data sets.

TABLE 1
H-ATLAS FIELDS

Name	Center	R.A. width[a]	Decl. width[a]
NGP ………	13 18 00, 29 00 00	15	10
GAMA A …..	09 00 00, 00 00 00	14	3
GAMA B …..	12 00 00, 00 00 00	14	3
GAMA C …..	14 30 00, 00 00 00	14	3
SGP A ……..	02 09 00, −32 54 50	11	6
SGP B ……..	23 15 36, −32 54 00	31	6

NOTE.—Columns are, from left: the name of the field; the central position of the field; the width of the field in degrees in R.A.; the width of the field in degrees in declination.

[a] The precise coverage of the fields and their orientation on the sky will depend on exactly when they are observed. See § 6 for more details.

surveys at shorter wavelengths, such as IRAS, are likely to underestimate the number of sources in the submillimeter band because these surveys miss the cold dust that radiates strongly at the longer wavelengths (Dunne & Eales 2001).

We have used two models to predict the properties of the sources that will be found in the H-ATLAS. First, the model of Lagache and collaborators (Lagache et al. 2003; Lagache et al. 2004) is an empirical evolution model in which an analytical form is assumed for the evolution, and the parameters of the model are adjusted to fit the observational data in the far-infrared and submillimeter wave bands, in particular the source counts at 24 μm, 70 μm, 160 μm, and 850 μm and the spectrum of the cosmic background radiation. Second, we have developed a new empirical evolution model based on the SCUBA Local Universe and Galaxy Survey (SLUGS; Dunne et al. 2000; Vlahakis et al. 2005). Both models give adequate agreement with the results of the BLAST survey (Dye et al. 2009), although the comparison between the results and the models is still at a preliminary stage because of the large amount of source confusion in the BLAST survey (Eales et al. 2009). We now describe the new model in more detail.

The model is based on the sample of 104 galaxies observed by Dunne et al. (2000) with the SCUBA submillimeter camera as part of SLUGS. These galaxies form a statistically-complete sample above a flux limit at 60 μm of 5.24 Jy (Dunne et al. 2000). All of these galaxies were detected at 850 μm and many at 450 μm. Dunne & Eales (2001) present a simple two-component dust model that fits the 60 μm, 100 μm, 450 μm, and 850 μm flux measurements. For the galaxies without measurements at 450 μm, it is possible to determine the parameters of the model by making the additional assumption that the temperature of the cold dust component is 20 K, which is the average of the estimates for the galaxies that do have complete flux measurements. The SLUGS sample is still the only large sample of galaxies for which there are empirical spectral energy distributions that extend from the far-infrared to the submillimeter wave bands. More sophisticated attempts to use the SLUGS data to predict the local luminosity function suggest that the simple method we present here leads to an underestimate of the local luminosity function (Vlahakis et al. 2005). However, the local submillimeter luminosity function is sufficiently uncertain that we are not too concerned about this—determining the luminosity function is one of the goals of the H-ATLAS—and the simple modeling method we present here has the advantage that it is possible to make predictions for the optical, radio and other properties of the galaxies we will detect with H-ATLAS.

We can use the SLUGS sample to predict the source counts in any submillimeter wave band in a straightforward way. Let us, for example, predict the number of sources in the SPIRE 250 μm band. If we assume "number-density evolution," in which the number of sources of a given luminosity changes with redshift, the number of sources above a given 250 μm flux density is

$$N(>S_{250\ \mu\mathrm{m}}) = \sum_{j=1}^{104} \int_0^{z(L_j, S_{250\ \mu\mathrm{m}})} \frac{E_d(z)}{V_j} dV, \qquad (1)$$

in which V_j is the comoving volume in which the jth SLUGS source could have been detected in the original survey from which it was selected and $E_d(z)$ is the evolution factor: the ratio of the comoving number-density of sources of a given luminosity at a redshift z to the comoving number-density at zero redshift. The upper limit of the integral is the maximum redshift at which the jth source could be placed and just be detected above the 250 μm flux limit. L_j is the luminosity of the jth SLUGS source, which can be estimated at the appropriate rest-frame wavelength at each redshift (for the observed wavelength of 250 μm) from the two-component dust model. If we assume that rather than number-density evolution we have luminosity evolution, in which the total number of galaxies stays the same but their luminosities evolve, the equation becomes:

$$N(>S_{250\ \mu\mathrm{m}}) = \sum_{j=1}^{104} \int_0^{z(L_j, S_{250\ \mu\mathrm{m}})} \frac{1}{V_j} dV. \qquad (2)$$

In this case, all the information about cosmic evolution is included in the upper limit because

$$L_j(z) = E_l(z) L_j(0), \qquad (3)$$

in which $E_l(z)$ is the evolution factor for luminosity evolution: the ratio of the luminosity of a galaxy at redshift z to the luminosity of the galaxy at zero redshift. These equations can be modified in a straightforward way to estimate the source counts at any submillimeter wavelength and also the cosmic background radiation in the far-IR and submillimeter wavebands.

In practice, we have used the simple luminosity-evolution model from Rowan-Robinson (2001), in which the rest-frame monochromatic luminosity over the entire far-IR/submillimeter wave band is assumed to evolve in the following way:

$$L(t) = L(t_0)\left(\frac{t}{t_0}\right)^P e^{Q(1-\frac{t}{t_0})} \tag{4}$$

in which t is the time from the big bang and t_0 is the time at the current epoch. P and Q are parameters of the model, and we found that $P = 3$ and $Q = 9$ produced acceptable fits to the spectral shape and intensity of the cosmic background radiation (Fixsen et al. 1998) and to the SCUBA 850 μm and *Spitzer* 70 μm source counts (Coppin et al. 2006, Frayer et al. 2006a, 2006b).

Table 2 shows the total number of sources that this model and the models of Lagache et al. (2003, 2004) predict should be detected by H-ATLAS, including the number at $z < 0.1$ and at $z < 0.3$. Figure 3 shows the redshift distributions predicted by the two models. The numbers of sources predicted by the models at the five wavelengths agree fairly well, although there are large differences between the predicted redshift distributions. These differences are not surprising because the observational data used to constrain the models consists almost entirely of number counts, which inform us about the numbers of sources in slices of the luminosity-redshift plane but nothing about the distribution of redshifts within each slice. Both sets of models do agree, however, in predicting that the H-ATLAS will detect a large number of sources in the relatively nearby universe ($z < 0.3$).

The advantage of the models based on SLUGS is that it is possible to predict the properties of the H-ATLAS sources in any wave band in which the spectral energy distributions (SED) of the SLUGS galaxies have been measured. For example, the number of H-ATLAS galaxies that are predicted to have B-band optical magnitudes in the range $B_1 < B < B_2$ is given by

TABLE 2

PREDICTIONS

Wavelength/redshift range	SLUGS	Lagache
110 μm, total	76944	65973
110 μm, $z < 0.1$	15489	7267
110 μm, $z < 0.3$	39695	18502
170 μm, total	68740	56351
170 μm, $z < 0.1$	10088	7049
170 μm, $z < 0.3$	26761	17883
250 μm, total	222061	170783
250 μm, $z < 0.1$	12500	13321
250 μm, $z < 0.3$	40073	34887
350 μm, total	50422	32636
350 μm, $z < 0.1$	2967	3192
350 μm, $z < 0.3$	7389	8170
500 μm, total	9734	6998
500 μm, $z < 0.1$	856	444
500 μm, $z < 0.3$	1714	1118

NOTE.—Columns are, from left: the wavelength and the redshift range (total means all redshifts); the prediction of the model based on the SCUBA Local Universe and Galaxy Survey (see text for details); the prediction of the Lagache model (Lagache et al. 2003, 2004).

$$N(B_1 < B < B_2) = \sum_{j=1}^{104} \int_{z_{\min}(B_1,B_2,S_{250\ \mu\mathrm{m}},L_j)}^{z_{\max}(B_1,B_2,S_{250\ \mu\mathrm{m}},L_j)} \frac{1}{V_j} dV, \tag{5}$$

in which the limits of the integral are the maximum and minimum redshifts at which the jth galaxy would fall both within the optical limits and above the 250 μm limit. In calculating these limits, we have generally assumed that the far-IR/submillimeter luminosity of the SLUGS galaxy is evolving with cosmic time in the way given by equation (4) but that its luminosity in the other wave band is not evolving. This assumption is almost certainly not correct, but given our lack of knowledge of the cosmic evolution in most wave bands it seems the safest (and simplest) one to make. It is also a conservative assumption, in the sense that the model probably underestimates how bright the H-ATLAS sources will be in the other wave bands. To use equation 5, it is necessary to have some information about the SEDs of the SLUGS galaxies in the relevant waveband, in this case the optical band. Similar equations to equation (5) can be written for any wave band.

Figure 4 shows the predictions for five wave bands Figures 4a and 4b show the predictions for the optical B and r bands. Several major redshift surveys have been based on catalogs defined in these bands and in § 4 we use our models to estimate the fraction of the H-ATLAS galaxies that will already have spectroscopic redshifts. In making the predictions for the B band, we used the B-band photometry that exists in the NASA Extragalactic Database (NED) for most of the SLUGS galaxies, and we made the assumption that all the SLUGS galaxies have an SED typical of an Sbc galaxy (Coleman et al. 1980). Note that although the assumption of a single optical SED for all SLUGS galaxies is a crude one, it should introduce little error at low redshift, where the observed and rest frames are very close in wavelength. We have made the r-band predictions using the V-band photometry that exists in NED for 75% of the SLUGS galaxies, with a small correction to the r band using the color transformations in Jester et al. (2005).

Figure 4c shows the predictions for the K-band. We have used the K-band photometry in NED that exists for almost all the SLUGS galaxies (mostly from 2MASS) and again assumed a standard Sbc SED.

Figure 4d shows the predicted 1.4-GHz continuum radio fluxes of the H-ATLAS galaxies. We have made the prediction for the continuum radio fluxes using the 1.4-GHz flux measurements that exist for almost all the SLUGS galaxies plus the assumption that all the SLUGS galaxies have a power-law radio continuum ($S \propto \nu^{-\alpha}$) with $\alpha = 0.7$. In this case, it seems quite likely that the assumption of no evolution in the radio wave band is incorrect because of the strong correlation between the far-infrared/submillimeter and radio emission from star-forming galaxies both at low and and high-redshift (Helou et al. 1986; Ibar et al. 2009). We have therefore assumed that radio luminosity also evolves in the way given by equation (4).

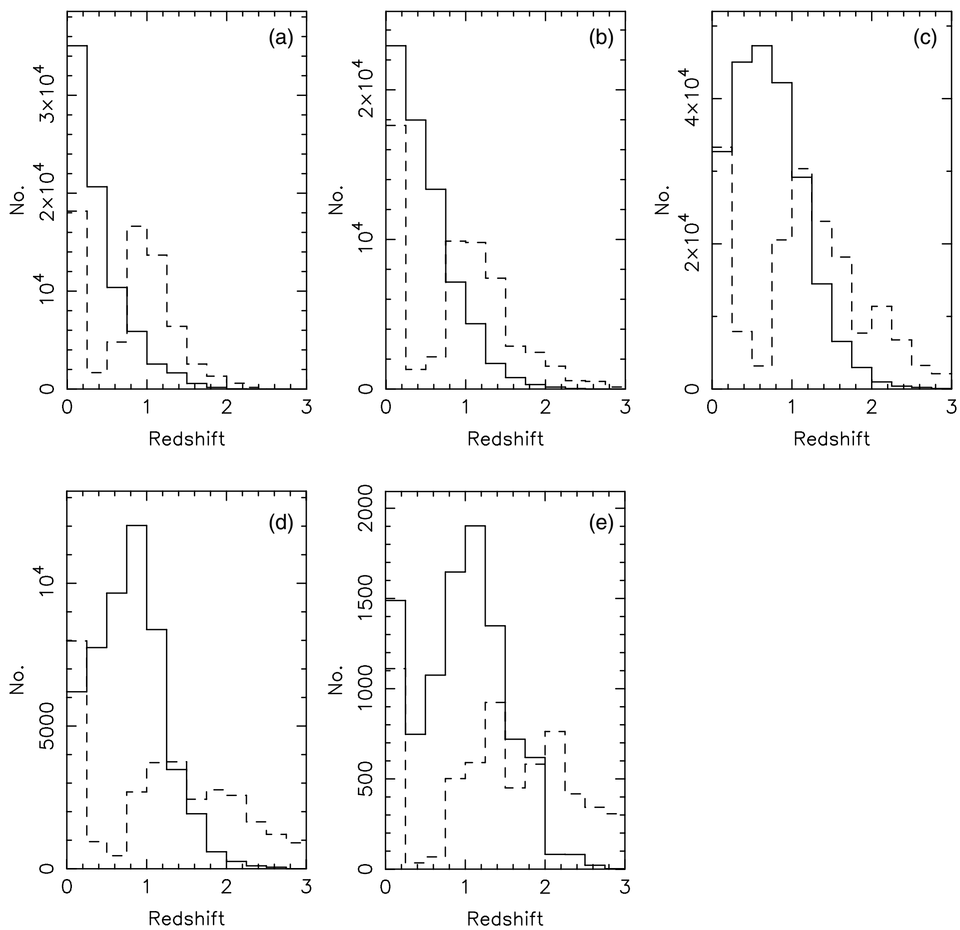

FIG. 3.—Redshift distribution predicted for H-ATLAS by the model described in the text (*solid line*) and the model of Lagache et al. (2003, 2004, *dashed line*).

Figure 4e shows the prediction for the H I line fluxes of the H-ATLAS galaxies. We used the H I line fluxes for the SLUGS galaxies given in NED. We have assumed that the amount of atomic hydrogen in a galaxy does not evolve, which may mean that the predicted H I line fluxes of the H-ATLAS galaxies are underestimates.

In all the panels of the figure, we have shown the detection limits of both existing and future surveys. The figure shows that, in contrast to the sources detected in the SCUBA surveys at 850 μm, it should be fairly easy to follow up the H-ATLAS sources with observations in other wave bands.

4. MULTI-WAVELENGTH DATA

We selected our fields partly because of the low "cirrus emission" from dust in our own galaxy (Fig. 2) but mainly because the complementary multiwavelength data are better than for any field of similar size. We describe here the multiwavelength data sets, both those that exist now and ones that are likely to soon exist.

4.1. Spectroscopy

There have been three major recent redshift surveys: SDSS (York et al. 2000); 2dFGRS (Colless et al. 2001) and GAMA (Baldry et al. 2009, Driver et al. 2009). The GAMA survey is still underway. All of the H-ATLAS fields are covered by one or more of these surveys. We have used the models from § 3 to predict the number of H-ATLAS sources that will already have redshifts from one of these surveys. In making these predictions, we have made the assumptions that (a) the 2dFGRS measured redshifts for 93% of the galaxies with $B < 19.6$ (Colless et al. 2001),[54] (b) that the SDSS measured redshifts for 94% of galaxies with $r < 17.77$ (Strauss et al. 2002), and (c) that GAMA will measure redshifts for all galaxies with $r < 19.4$ (Driver et al. 2009). Table 3 lists the predicted numbers of sources which will already have spectroscopic redshifts in the different

[54] We have made the transformation from the b_j magnitude system using the relationship $b_j = B - 0.28(B - V)$ given in Maddox et al. (1990).

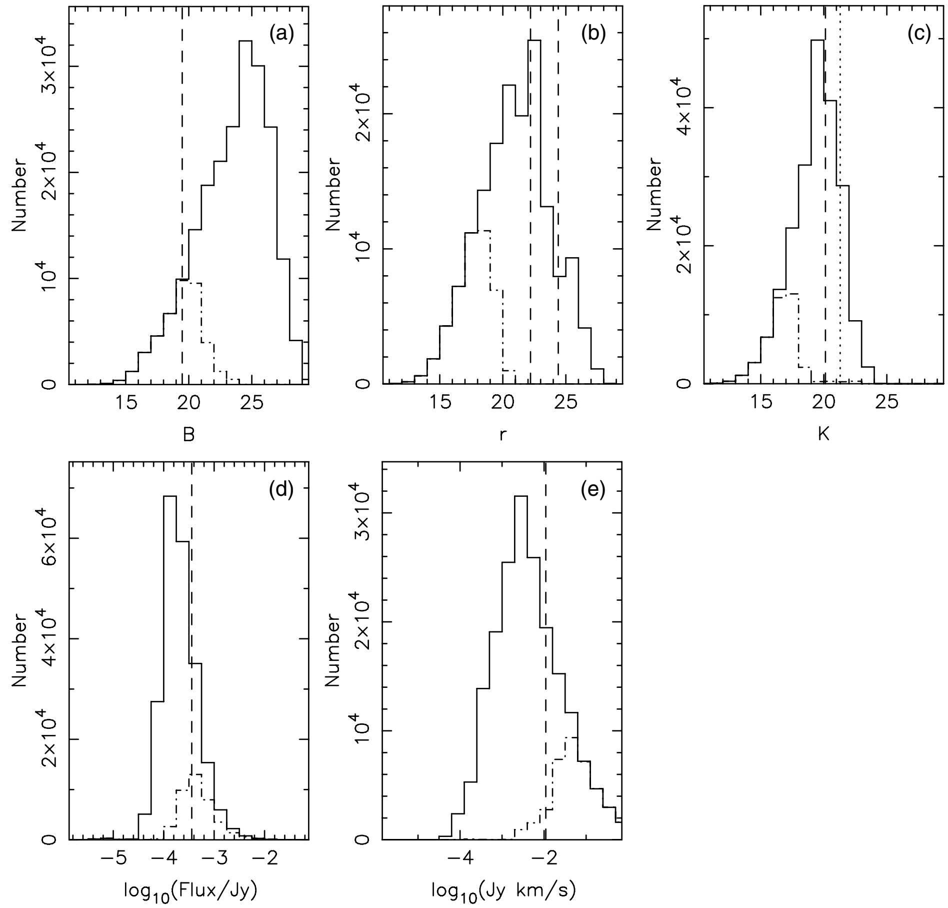

FIG. 4.—Predicted distribution of flux or magnitude for the H-ATLAS survey in different wave bands using the method described in § 3: (*a*) optical B band; (*b*) optical r band; (*c*) near-infrared K-band; (*d*) radio (1.4 GHz); (*e*) 21 cm line. In each figure, the *solid line* shows the prediction for the whole survey and the *dot-dashed line* shows the prediction for the sources at $z < 0.3$. *Vertical dashed lines* show the flux or magnitude limit for these current or future surveys: B band—2dFGRS; r band—imaging part of SDSS (*left*) and ESO KIDS survey (*right*); K band—Large Area Survey (*left*), which is part of the UKIRT Infrared Deep Sky Survey (Warren et al. 2007), and ESO VIKING survey (*right*); radio—our GMRT 325 MHz survey, translated to 1.4 GHz using the assumption of a power-law radio spectrum (S $\propto \nu^{-\alpha}$) with $\alpha = 0.7$ (§ 4.3); H I—the strawman survey described in § 4.3.

fields. The table shows that ~2×10^4 H-ATLAS galaxies are likely to already have spectroscopic redshifts, and that the percentage of H-ATLAS galaxies at $z < 0.1$ with spectroscopic redshifts is likely to be very high. All three surveys, of course, contain far more information about the galaxies than only the redshifts, such as measurements of line ratios, line equivalent widths, kinematics etc.

4.2. Imaging from the Ultraviolet to the Near-Infrared

At ultraviolet wavelengths, approximately half of the total survey area has been observed with the *Galaxy Evolution Explorer* (*GALEX*). This has mostly been part of the *GALEX* Medium Imaging Survey (MIS), which has an exposure time of 1500 s and a limiting AB magnitude of $\simeq$23. We and the GAMA team have been awarded time for a proposal to complete the GALEX coverage of the GAMA fields to the MIS depth (P.I. Tuffs).

In the optical wave band, the GAMA fields and the NGP field have been surveyed in five passbands by the SDSS. The limiting magnitude of the r-band imaging is shown in Figure 4b. As yet, the SGP field has only been surveyed with the UK Schmidt Telescope using photographic plates. In the next three years, the H-ATLAS fields should be covered by three new optical surveys. The GAMA and SGP fields will be observed in 4 optical passbands as part of the Kilo Degree Survey (KIDS), an ESO public survey that will be carried out with the VLT Survey Telescope (VST). The sensitivity limits of KIDS will be about 2 mag fainter than the SDSS limits. The NGP and GAMA fields will be observed in 5 bands by Pan-STARRS1 and the SGP and GAMA fields will be observed in 6 bands by SkyMapper (Keller et al. 2007). The approximate

TABLE 3
REDSHIFT SURVEYS

H-ATLAS Field	Data Sets	No. at $z < 0.1$	No. at $z < 0.3$
NGP	SDSS	3366 (2895)	10865 (4563)
GAMA	GAMA, SDSS, 2dFGRS	3366 (3366)	10865 (9456)
SGP	2dFGRS	5610 (4993)	18106 (8148)
All fields	...	12342 (11254)	39833 (22167)

NOTE.—Columns are, from left: the H-ATLAS fields; the redshifts surveys covering this field; the predicted number of sources at $z < 0.1$ in this field with the predicted number with spectroscopic redshifts in parentheses; the predicted number of sources at $z < 0.3$ in this field with the predicted number with spectroscopic redshifts in parentheses.

5σ limits for all the optical surveys are given in Table 4. A little further off in time, the SGP field will be observed as part of the Dark Energy Survey.[55]

In the near-infrared, the GAMA and NGP fields are being surveyed in 4 passbands as part of the Large Area Survey (LAS), a legacy survey being carried out as part of the UKIRT Infrared Deep Sky Survey (Warren et al. 2007). The GAMA and SGP fields will soon be observed in five passbands as part of the VISTA Kilo-Degree Infrared Galaxy Survey in the Infrared (VIKING), an ESO public survey that is currently being carried out with the Visible and Infared Telescope for Astronomy (VISTA). The approximate limits of both surveys are given in Table 4 and shown in Figure 4c.

4.3. Radio Surveys: Continuum and H I

The H-ATLAS fields have been surveyed at 1.4 GHz as part of the NRAO VLA Sky Survey. This survey is not sensitive enough, however, to detect a significant percentage of the H-ATLAS sources. We are therefore currently completing a radio survey (P.I. Jarvis) of the GAMA fields at 325 MHz with the Giant Metrewave Radio Telescope (GMRT), which will reach an approximate 5σ sensitivity of 1 mJy. The limit of this survey is shown in Figure 4d. The NGP field is also high on the list of targets for an early survey with the Low Frequency Array for Astronomy (LOFAR).

There is currently no H I survey of any of the H-ATLAS fields that could yield H I measurements of a significant fraction of the H-ATLAS sources. However, the SGP and GAMA fields are natural targets for the new southern radiotelescopes that are being built as prototypes for the Square Kilometre Array (and for the SKA itself, of course). We have designed a potential H I survey of the SGP field using the parameters given for the Australian Square Kilometre Pathfinder Array (ASKAP) by Johnston et al. (2007). We estimate that in one month of observing time it should be possible to carry out a survey of the SGP sensitive to galaxies out to $z \simeq 1$ with an approximate sensitivity to H I flux of $\simeq 10^{-2}$ Jy km s^{-1} (Fig. 4e).

[55] See www.darkenergysurvey.org.

4.4. Planck and Other Telescopes

The Planck Surveyor is surveying the whole sky in nine passbands, two of which (350 and 550 μm) are nearly the same as those that are being used in H-ATLAS. The size (FWHM) of the Planck beam is $\simeq 10$ times greater than that of H-ATLAS at the same frequency, although the sensitivity in surface brightness is fairly similar. Therefore, in the common area of sky (one-eightieth of the whole sky), the two surveys will be complementary, with the H-ATLAS providing high-resolution observations of the sources that will be detected by Planck.

The SGP field may also be observed by the South Pole Telescope, a telescope designed to look for high-redshift clusters using the Sunyaev-Zeldovich effect.

5. THE H-ATLAS SCIENCE PROGRAM

In this section we describe the six major science programs planned by the H-ATLAS team. We note that these programs represent only a limited subset of the scientific projects that will be ultimately possible with the H-ATLAS, for two reasons. First, many other projects will become possible as the surveys of the H-ATLAS fields at other wavelengths (§ 4) are gradually completed. Second, since the wavelength range from 200–500 μm is virtually unexplored and since the H-ATLAS will cover one-eightieth of the sky in this wave band, it is possible that there will be some unanticipated discoveries.

5.1. The Local Universe

Our models (§ 4) predict that the H-ATLAS will detect $\simeq 40{,}000$ galaxies in the relatively nearby universe ($z < 0.3$). Almost all of the galaxies detected at $z < 0.1$ and approximately half of the galaxies detected at $z < 0.3$ should already have spectroscopic redshifts. Most of these galaxies will be unresolved by the H-ATLAS beams. There are $\simeq 120$ clusters of Abell richness class 1 or greater, including the Coma Cluster, in our fields.

Apart from providing the spectroscopic redshifts necessary to calculate the intrinsic properties of the sources (luminosities, dust masses, etc.), the complementary data will be helpful in other ways. Three are particularly important. First, the redshift surveys will allow us to determine the position within the cosmic web of each Herschel galaxy and to measure the density of the galaxy's environment (exactly how to do this best is debatable—e.g., Balogh et al. 2004). Second, the existence of catalogs at other wavelengths means that the H-ATLAS will contain more information than the individual source detections. By coadding ("stacking") the *Herschel* emission at the positions of objects in different classes, we can study the dust and dust-obscured star formation in objects that would be too faint to detect individually (Dole et al. 2006; Dye et al. 2007b).

TABLE 4
Optical and Near-Infrared Data

H-ATLAS Field	Data Sets	u	v	g	r	I	z	Z	y	Y	J	H	K
NGP	SDSS	22.0	…	22.2	22.2	21.3	20.5	…	…	…	…	…	…
NGP	Pan-STARRS1[a]	…	…	24.1	23.5	23.4	22.4	…	21.2	…	…	…	…
NGP	LAS	…	…	…	…	…	…	…	…	20.87	20.55	20.28	20.13
GAMA	SDSS	22.0	…	22.2	22.2	21.3	20.5	…	…	…	…	…	…
GAMA	KIDS	24.0	…	24.6	24.4	23.4	…	…	…	…	…	…	…
GAMA	Pan-STARRS1[a]	…	…	24.1	23.5	23.4	22.4	…	21.2	…	…	…	…
GAMA	SkyMapper[b]	22.9	22.7	22.9	22.6	22.0	21.5	…	…	…	…	…	…
GAMA	LAS	…	…	…	…	…	…	…	…	20.87	20.55	20.28	20.13
GAMA	VIKING	…	…	…	…	…	…	23.1	…	22.4	22.2	21.6	21.3
SGP	KIDS	24.0	…	24.6	24.4	23.4	…	…	…	…	…	…	…
SGP	SkyMapper[b]	22.9	22.7	22.9	22.6	22.0	21.5	…	…	…	…	…	…
SGP	VIKING	…	…	…	…	…	…	23.1	…	22.4	22.2	21.6	21.3

Note.—Columns are, from left: the H-ATLAS field; the optical or near-IR survey; the quoted sensitivity limits in AB magnitudes for the passbands used in the survey (these are 5σ limits for point sources, except in the case of the SDSS, for which the limits represent the 95% detection repeatability for point sources).

[a] The limits are for the planned 3 yr survey with Pan-STARRS1.

[b] The limits are for the planned 6 epoch survey by SkyMapper.

An important example is elliptical galaxies (§ 1). Third, we will be able to answer the question of what fraction of the optical light from a galaxy is obscured by dust. Optical astronomers have struggled with this issue for 50 years (Holmberg 1958; Davies & Burstein 1995) with limited success, largely because optical galaxy catalogs have large selection effects caused by dust. The implications for extragalactic astronomy are potentially large, with a recent study concluding that the optical luminosity function is significantly altered by dust extinction and that even bulges suffer as much as 2 mag of extinction at certain inclinations (Driver et al. 2007). The ultraviolet, optical, and near-infrared data that exist for some of the fields (§ 4) will allow us to address this issue by the simple energy-balance technique of comparing the total dust emission to the total unobscured starlight. The only assumption in this technique is that the absorption by the dust is isotropic. This is almost certainly untrue, but by averaging over many objects we can largely eliminate the effects of anisotropy (Driver et al. 2008).

For this program we give the following four projects as examples:

1. We will make the first accurate estimate of the local submillimeter luminosity and dust-mass functions down to dust masses of ~$10^{4.5}$ $M_\odot$ (Fig. 5). As we will have Herschel measurements for $\simeq 10,000$ galaxies at $z < 0.1$, we will be able to compare the luminosity and dust-mass functions for different classes of galaxy (e.g., different Hubble types, high and low environmental density, etc.). We will also be able to extend the study of the luminosity and dust-mass functions to higher dimensions, for example by examining how the space density of galaxies depends on both dust mass and stellar mass.

2. Using the results from the redshift surveys, we will investigate how the dust-obscured star formation depends on the local and large-scale environment. This will complement previous optical studies (Balogh et al. 2004; Kauffmann et al. 2004), because our observations will be much more sensitive to starbursts, which may well have a different environmental dependence from quiescent star formation.

3. We will investigate how the dust content of the universe and dust-obscured star formation have changed during the last three billion years. This will finally follow up an important discovery from IRAS that there is strong evolution in the luminosity function at a surprisingly low redshift (Saunders et al. 1990), a phenomenon which also may have been seen in the SDSS (Loveday et al. 2004).

4. One of the strongest correlations in astronomy is that between the far-infrared and nonthermal radio emission of galaxies (Helou et al. 1986; Ibar et al. 2009). A widely-accepted explanation is that both the far-infrared emission and the radio emission are ultimately caused by young stars, with the far-infrared emission being from the dust heated by the young stars and the radio emission being nonthermal emission from the relativistic electrons generated in the supernova remnants produced when the stars reach the end of their lives. Nevertheless, many of the properties of this relationship are hard to explain, in particular the approximate unity slope when the two quantities are plotted on logarithmic axes (Vlahakis et al. 2007). By investigating this relationship as a function of environment, redshift, star-formation activity, and other properties, we will try to understand better its fundamental cause.

5.2. Planck Point Sources and Diffuse Emission

The Planck High-Frequency Instrument (HFI) will survey the whole sky in six bands (3 mm, 2.1 mm, 1.4 mm, 0.85 mm, 0.55 mm, 0.35 mm), the first survey of the whole sky at these wavelengths. Apart from its measurements of the primordial cosmic background radiation (CMB), the HFI will detect

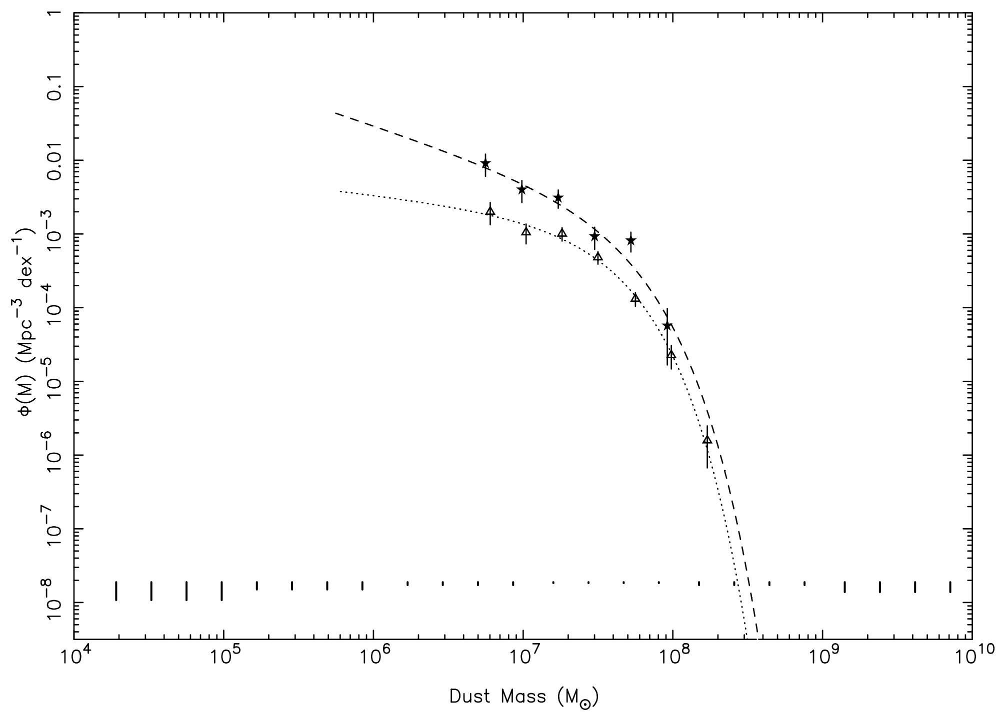

FIG. 5.—*Triangles* and *stars* show estimates of the dust-mass function (the space-density of galaxies as a function of dust mass) from Vlahakis et al. (2005). See that article for an explanation of the symbols. *Vertical lines* across the bottom show our estimates, on the assumption of Poisson statistics, of the $\pm 1\sigma$ errors on the estimate of the dust-mass function from the H-ATLAS.

extended foreground emission, such as dust in the Galaxy. It is also likely to detect many point sources (de Zotti et al. 2005), including nonthermal radio sources, thermal dust emission from nearby galaxies, and Sunyaev-Zeldovich (SZ) sources associated with distant clusters, the consequence of the scattering of the CMB radiation by the electrons in the intracluster medium.

The SZ sources detected by Planck are potentially of great importance for cosmologists, because the number-density of clusters as a function of redshift depends critically on the cosmological model (Bartelmann 2001; Bartelmann et al. 2002). It might also be possible, because the spectral shape of the SZ effect depends on the peculiar motion of the cluster, to measure bulk flows in the universe (Kashlinsky & Atrio-Barandela 2000), which is another critical test of the cosmological paradigm. A major problem, however, is the contamination of the SZ effect by thermal emission from dusty galaxies within the large (5′–10′) Planck beam, because there is evidence that even at moderate redshift the combined emission from dust in cluster galaxies is comparable to the SZ effect in the 0.85 mm band, and much greater in the two shorter wavelength bands (Zemcov 2007). There is zero SZ effect at 1.4 mm, which leaves only the two long-wavelength bands with little contribution from dusty galaxies, but as these also have the worst angular resolution, there is the additional problem of confusion with nonthermal radio sources.

The H-ATLAS will survey one-eightieth of the sky in the two Planck bands with the highest frequencies, but with much better resolution. The sensitivity to extended regions of low surface brightness is likely to be similar for the two surveys. The combination of the two surveys will make possible several joint projects:

1. The effects of confusion on the Planck point source catalog are likely to be large, particularly in the highest frequency channels. These include Eddington bias (Eddington 1940), which can lead to both overestimates of the fluxes of the sources and spurious detections, as well as a large and uncertain effect on the positions of the sources. The H-ATLAS will provide a sample of sources with accurately known positions and fluxes, which can then be checked against the Planck point-source catalog for the two highest-frequency channels from the same area of sky. This comparison will provide an estimate of the correction factor for the Planck fluxes, an estimate of the fraction of the Planck sources that are spurious, and measurements of the positional errors of the Planck sources.

2. Some of the Planck science goals, such as the detection of anisotropies in the cosmic infrared background (Lagache et al. 2003, 2004), require the successful removal of galactic cirrus emission. The galactic cirrus should be easier to distinguish in the H-ATLAS images because of the better angular resolution, and so we will be able to test the Planck component separation techniques.

3. The combination of the high-resolution images provided by H-ATLAS and the spectral energy distributions of the Planck sources should make it possible to determine unambiguously the nature of each source in the overlap region between the two surveys. The detailed information provided by the H-ATLAS for the Planck sources in this region will make it possible to develop better statistical methods, based on their spectral energy distributions, for determining the nature of the Planck sources in the region not covered by H-ATLAS.

4. In the overlap region between the two surveys, the H-ATLAS will make it possible to determine the contribution of dusty galaxies to each potential SZ source and then subtract these galaxies' emission from the total signal. The detailed information in the overlap region will also provide statistical information about the average level of contamination for the Planck SZ sources not covered by H-ATLAS.

5.3. The H-ATLAS Lens Sample

In principle, gravitational lensing is a powerful way of investigating the evolution in the density profiles of galaxies, a fundamental test of models of structure formation. In practice, it has proved very hard to assemble the necessary large sample of lenses. The most ambitious program to date searched for lenses among flat-spectrum radio sources but, after high-resolution radio observations, found only 22 lenses out of 16,000 radio sources—a success rate of 0.14% (Browne 2003).

Submillimeter surveys are possibly the ideal way to find lenses. At $z \geq 1$, the monochromatic flux density at the long-wavelength end of the submillimeter wave band depends on luminosity but is approximately independent of redshift, a consequence of the characteristic spectral energy distribution of dust in galaxies. A result of this and the strong cosmic evolution in the submillimeter wave band is that sources in submillimeter surveys tend to lie at high redshifts (§ 1) and are thus likely to have a large optical depth to lensing. Because of the approximate independence of flux and redshift at $z \geq 1$, a bright source in a submillimeter survey must necessarily have a high luminosity (unless it is at $z \leq 1$). Above a critical flux density, any sources are highly likely to be lensed systems because their measured luminosities will be greater than the rapid falloff in the (unlensed) luminosity function.

The model in Figure 6, for example, predicts that at $S_{500\mu m} >$ 100 mJy the sources will be a mixture of lensed high-redshift galaxies, nearby galaxies, and flat-spectrum radio sources (Negrello et al. 2007). Since the latter two catagories should be easy to remove (from the presence of a bright galaxy or by looking at the SED in the submillimeter wave band), the lens yield of such a sample would be close to 100%. These models predict that the H-ATLAS will contain ~1500, 800, and 350 strongly-lensed galaxies at 250 μm, 350 μm, and 500 μm, respectively.

This is the only one of the H-ATLAS science programmes for which follow-up observations will be essential, both to determine whether a bright 500 μm source is indeed a lensed system and to scientifically exploit the resulting sample of lenses. Fortunately, a source with $S_{500\mu m} \sim 100$ mJy would be easy to map; a 30 minute observation with the Submillimetre Array, a 1 hr observation with the VLA, or a $\simeq$1 minute observation with ALMA would be enough to confirm a source as a lens and to map the image structure. The prediction that large-area submillimeter surveys are the ideal way to construct large samples of lenses may not be correct, but if it is, there are many possible uses for a large sample of lenses. These include:

1. An investigation of the evolution of the density profiles of the lenses (probably mostly elliptical galaxies). In principle, it should be possible to use standard techniques (Dye et al. 2007a)

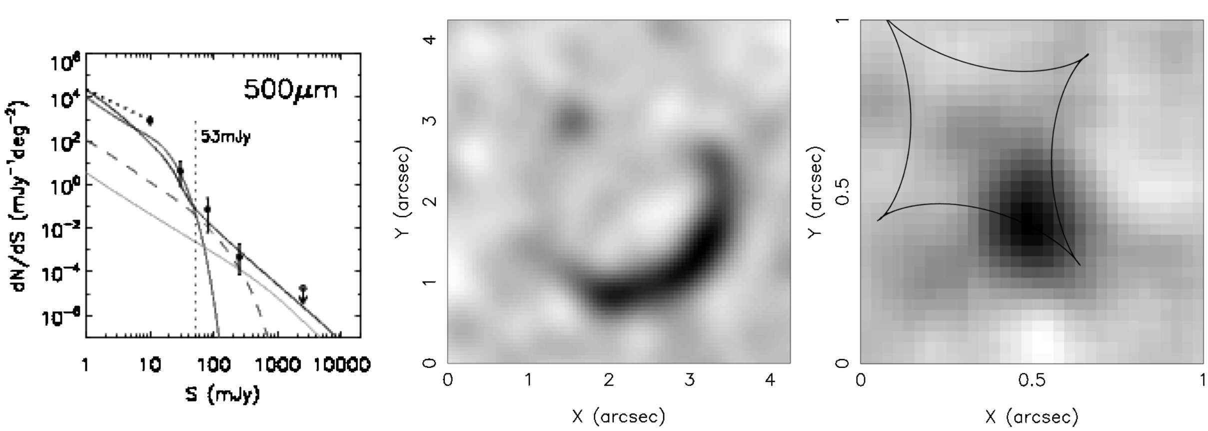

FIG. 6.—*Left panel* shows the predicted number of sources as a function of 500 μm flux density plotted over the results from BLAST (Negrello et al. 2007). The *vertical dashed line* shows the approximate limit of H-ATLAS at 500 μm. See the electronic edition of the PASP for a color version of this figure.*Middle panel* shows a simulated image of a strongly lensed 100 mJy 500 μm H-ATLAS source as observed using the Submillimetre Array at 870 μm. *Right panel* shows the reconstructed source obtained by applying the reconstruction method of Dye et al. (2007a) to the simulated ring image. The image caustic of the best fit lens model is overplotted.

to reconstruct separately the structures of the dark-matter halo and of the baryonic component of each lens.

2. A study of the structures of high-redshift dust sources by reconstructing the original (unlensed) structure of the source (Fig. 6). Since our systems are lensed, we will be able to study galaxies well below the Herschel confusion limit (Smail et al. 1997).

5.4. Active Galactic Nuclei

The discovery that most nearby galaxies contain a black hole, with the mass of the black hole being strongly correlated with the mass of the surrounding spheroid of stars (Magorrian et al. 1998), was possibly one of the most important discoveries in extragalactic astronomy in recent years, because it implies the formation of the stars and of the central black hole in a galaxy are connected. Previous submillimeter observations of high-redshift quasars have detected $\simeq 5\%–10\%$ of these objects (Priddey et al. 2003; Beelen et al. 2006), and the spectral energyy distributions of the detected quasars imply that most of the submillimeter emission must be coming come from a starburst surrounding the active nucleus rather than directly from the nucleus itself. This supports the idea that the formation of the stars and the formation of the central black hole in a galaxy are connected.

We will use the H-ATLAS to detect both individual active galactic nuclei that fall in our fields and to carry out statistical analyses of AGN that are too faint to detect individually by coadding the Herschel emission at the positions of all the AGN in a given class. Let us consider as an example Type 1 quasars. Figure 7 shows quasars drawn from the Palomar Green (PG) survey and the SDSS as a function of redshift and optical luminosity. Because of the strong correlation between luminosity and redshift in any flux-limited sample, it is crucial to observe more than one sample, so that one can compare quasars with the same optical luminosity at different redshifts and vice versa. The detection rate of PG quasars by IRAS and ISO is $\simeq 80\%$ (Haas et al. 2003). We will use the H-ATLAS to extend the far-IR/submillimeter study of quasars to the more distant SDSS quasars, of which there are $\simeq 10^4$ in the H-ATLAS fields. Using the results of a pilot study with the *Spitzer* legacy survey SWIRE (Serjeant et al. 2009), we estimate that we will detect $\simeq 440$ quasars at $z < 3$ and $\simeq 210$ quasars at $z > 3$. This is $\simeq 15$ times greater than the number of existing detections of high-redshift quasars. We will investigate the properties of the quasars that are too faint to detect individually by a stacking analysis.

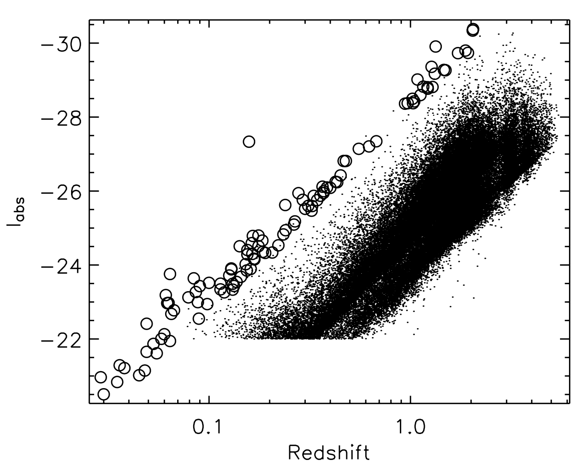

FIG. 7.—Distribution of PG (*open circles*) and SDSS (*points*) QSOs as a function of redshift and absolute I-band magnitude.

5.5. Large-Scale Structure

The H-ATLAS will detect ∼$200,000$ sources with a median redshift of ∼1 and will therefore contain a large amount of information about large-scale structure up to a scale of $\simeq 1000$ Mpc at $z \sim 1$. Many large-scale–structure projects, such as searches for baryonic oscillations, will only become possible in the future, as the near-IR (VIKING, UKIDSS) and optical (KIDS, Pan-STARRS, the Dark Energy Survey) surveys eventually provide photometric redshift estimates for most of the sources. There are two projects that are possible immediately:

1. The H-ATLAS will make possible measurements of the angular correlation function on very large scales. These measurements will make it possible to discriminate between some models of galaxy formation. Figure 8, for example, shows the results of using a Monte Carlo simulation to predict the amplitude of the angular correlation function of H-ATLAS sources using three alternative models of galaxy formation: the hybrid model from Van Kampen et al. (2005) and two new models (Van Kampen et al., in preparation). The simulation shows that it should be easy to discriminate between these models.

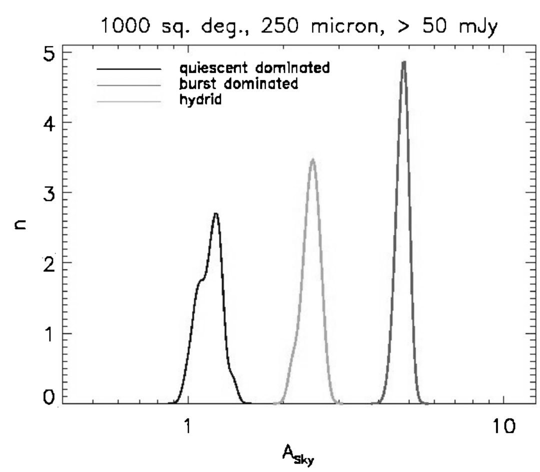

FIG. 8.—Histogram of the amplitude of the angular correlation function ($A_{\rm sky}$) of H-ATLAS sources for 100 Monte Carlo realizations for each of three different models of galaxy formation: the hybrid model described by Van Kampen et al. (2005) and two new models (Van Kampen et al., 2010 in preparation). See the electronic edition of the PASP for a color version of this figure.

2. The individual sources, however, only represent $\simeq 10\%$ of the extragalactic background radiation at the Herschel wavelengths and the unresolved background contains a wealth of further information about the clustering properties of dusty galaxies. A powerful technique to extract further information is to investigate the clustering properties of the intensity distribution on the maps after the high signal-to-noise sources have been removed (Amblard & Cooray 2007; Lagache et al. 2007). The strength of the fluctuations on large angular scales (linear regime) can be used to estimate the average mass of the dark-matter halos containing the sources, whereas the strength of the fluctuations on small angular scales (nonlinear regime) can be used to estimate the halo-occupancy distribution (Amblard & Cooray 2007).

5.6. Galactic Dust Sources

We will use the H-ATLAS to look for dust associated with stars, especially debris disks and dust around stars on the asymptotic giant branch. We will also study the distribution and spectral properties of dust in the interstellar medium. Although the H-ATLAS fields are at high galactic latitudes, in order to minimize the emission from dust within the Galaxy, IRAS images show that there is plenty of dust even at the Galactic poles (Fig. 9). The H-ATLAS will allow us to study the structure of interstellar dust on an angular scale $\simeq 10$ times smaller than was possible with IRAS (Mivilles-Deschenes et al. 2007) and will be possible with Planck, while still having as good sensitivity to large-scale structure as the two other telescopes. The H-ATLAS will also detect the cold dust missed by IRAS.

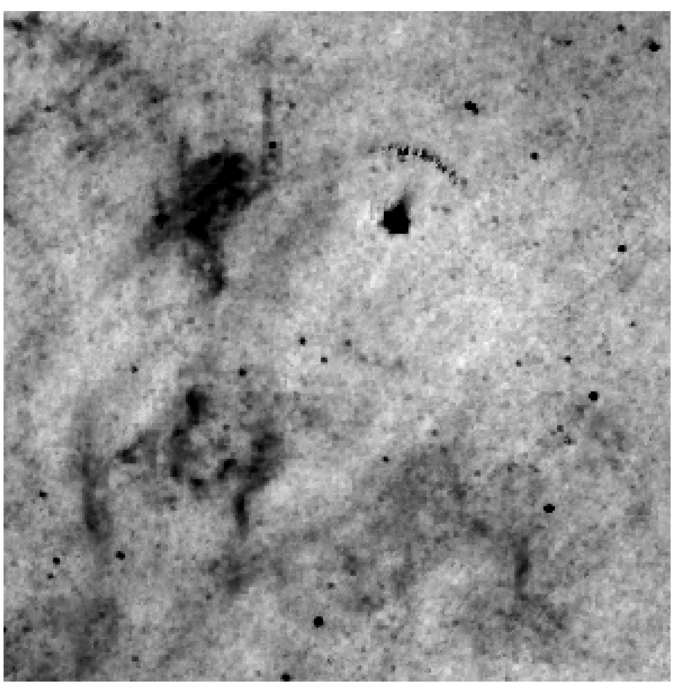

FIG. 9.—IRAS image at 100 μm of a 10×10 deg^2 region around the SGP.

A more speculative idea is to look for prestellar cores and protostars at high latitudes. Since the dust disks in galaxies are thin, most of the high-latitude dust is within 0.5 kpc. Therefore, we will be able to carry out a search for prestellar cores and protostars in our fields down to surprisingly low mass limits. On the assumption of a dust temperature of 20 K and a standard gas-to-dust ratio, we estimate that we should detect all protostars and prestellar cores down to a mass of ~0.002 $M_\odot$—well below the brown dwarf limit and in the Jupiter regime.

6. FURTHER TECHNICAL DETAILS AND DATA RELEASE

The basic parameters of the survey were given in § 2. In this section, we describe some technical issues that will affect the nature of the data that we eventually release to the community.

An important feature of the survey is that we plan to observe all fields twice. The main purpose of this is to overcome the potential problem of low-frequency (l/f) noise, caused by either slow drifts in the temperatures of the detectors or other changes in the instrument electronics. These drifts in time can lead to spurious large-scale structure in the final maps, which would be a problem for some of our science projects. As long as the two sets of observations are in different directions, however, it should be possible to use mapping algorithms such as MADmap (Cantalupo et al. 2010) to produce maximum-likelihood images of the sky that are free of the effects of this noise. Simulations suggest that as long as the scan direction of the two sets of observations is separated by at least 20°, there should be no features in the final maps caused by these drifts (Waskett et al. 2006).

Achieving two sets of observations with different scan directions, however, is quite tricky, partly because of the severe constraints on the way that *Herschel* will observe the sky and partly because of the sheer size of H-ATLAS (11% of the time available for open-time key projects). Surveys will be carried out with *Herschel* by using the telescope to scan across the sky along a great circle, then moving the telescope a short distance in a perpendicular "cross-leg" direction, and then moving the telescope back along a great circle, thus gradually building up a map of the sky. A complication of observing with SPIRE is that the SPIRE bolometers do not instantaneously fully sample the sky, and so to produce a fully-sampled SPIRE image it is necessary to carry out the scan in one of 24 possible directions that are related to the sixfold symmetry of the array (there is not a similar constraint for PACS because it is a fully-sampled array). Other complications are that it is necessary to keep the Sun safely behind the telescope's sun shield and that it is only possible to rotate the telescope completely around one axis. Waskett et al. (2007) give a good introduction to the complications of carrying out surveys with *Herschel*. The result of these constraints is that it is only possible to observe a given field during certain visibility windows, the duration of which depends on the position of the field.

The easiest fields to observe are the GAMA fields, which have long visibility windows because they are the ones closest to the ecliptic plane. The Astronomical Observation Requests (AOR), the units out of which the telescope's observing program is built, of the GAMA fields each consist of two sets of observations with orthogonal scan directions of an area of sky $\simeq 4 \times 4\ \mathrm{deg}^2$. These AORs, which will take approximately 16 hr to complete, will result in approximately square images, like those shown in Figure 2, although the orientation of the square will depend on the exact time at which the observation is made. Thus the coverage within each square will be uniform but we cannot predict now the angle that each square will make to the celestial equator, and thus the precise overlap with the area covered by the surveys in other wave bands (§ 4).

The other two fields are more difficult to observe because they have shorter visibility windows and because we need to map large contiguous areas of sky to make the best use of the complementary data in other wave bands. As an example, we will consider the larger of the fields near the SGP. To make the best use of the redshifts from the 2dF Galaxy Redshift Survey, the field has a small range of declination but a large range of right ascension (Fig. 2). For this field, the individual AORs each contain one set of observations with a single scan direction. Figure 10 shows the layout of the AORs, although their exact orientation depends on exactly when the observations are done. The scan directions are either roughly along lines of constant declination, with the observations covering a rectangular area of $\simeq 3°$ in declination and $\simeq 12°$ in right ascension, or roughly along lines of constant right ascension, with the observations covering a rectangular area of $\simeq 6°$ degrees in declination and $\simeq 4°$ in right ascension. We have set some constraints on when the AORs are observed to avoid the rectangles being rotated too far from a north-south line but it is not possible to make the constraints too severe because of the difficulty of scheduling such a large program. Figure 11 shows an example of the coverage we are likely to have for this field. The full range of the exposure time shown by the color table is a factor of 4, so the sensitivity in the apparent gaps is a factor of $\simeq 2$ worse than in the places where we have the best coverage. Apart from in these gaps, every point in the field will have at least two sets of observations, with the scans in approximately orthogonal directions, and thus we will be able to use maximum-likelihood imaging algorithms to remove the effect of 1/f noise. Figure 10 also shows the design of the AORs for the field near the NGP. The individual AORs again each contain one set of observations with a single scan direction. There are two sets of AORs with roughly orthogonal scan directions, each covering a rectangular area of $\simeq 9° \times 4°$ with the longer side in the scan direction. The orientation of the overall field and the coverage within the field are still uncertain and will depend on the final telescope schedule. For all fields, one of the legacy data products will be coverage maps of the fields.

A useful byproduct of our observing strategy of two sets of observations of each point within a field is that we will be able to look for time-varying and moving objects in the H-ATLAS data. Because of the scheduling difficulties, we have not placed any constraint on the time interval between two observations of the same place within the SGP and NGP fields, and thus it is only within the GAMA fields that we will have two sets of observations separated in time by a roughly constant interval. This interval is approximately 8 hr, which is well suited for looking for asteroids but not, for example, for objects in the Edgeworth-Kuiper Belt.

We intend to release the H-ATLAS data (maps and catalogs) to the community in a series of data releases. The first data release will be for a $4° \times 4°$ area within the 9 hr GAMA field (Table 1), which was observed during the Herschel Science Demonstration

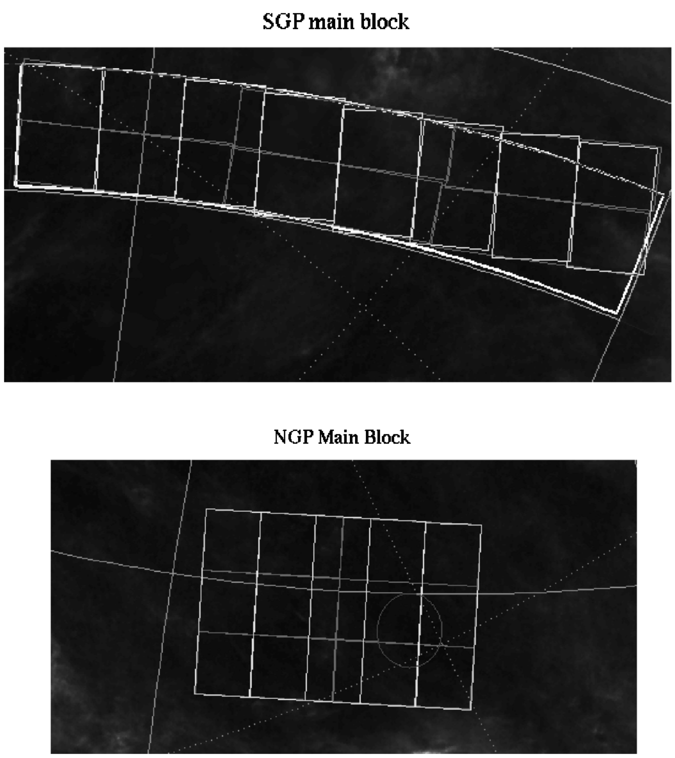

FIG. 10.—Design of the surveys of the ATLAS NGP field and of the larger of the two SGP fields. See the electronic edition of the PASP for a color version of this figure.

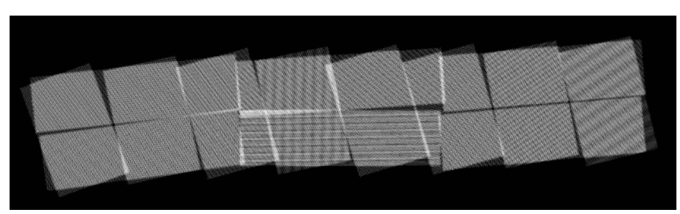

FIG. 11.—Simulation of the likely coverage of the larger of the fields near the SGP. The range of exposure time shown by the color table is a factor of 4. See the electronic edition of the PASP for a color version of this figure.

Phase (2009 October 15–November 30). We currently expect to release the maps and catalogs for this region in 2010 June. The complexity of telescope scheduling means that we cannot yet give a firm date for the next data release. More information can be found on the Herschel ATLAS website.[56]

7. CONCLUSIONS

The Herschel ATLAS is the largest open-time key program that will be carried out with the *Herschel Space Observatory*. It will survey 570 deg^2 of the extragalactic sky, 4 times larger than all the other Herschel extragalactic surveys combined, in five far-infrared and submillimeter bands. We have described the survey, the complementary multiwavelength data sets that will be combined with the Herschel data, and the six major science programmes we plan to undertake. Using new models based on a submillimeter survey of nearby galaxies, we have presented predictions of the properties of the sources that will be detected by the H-ATLAS. We intend to release the H-ATLAS data—maps and catalogs—to the astronomical community in a series of data releases. The first of these will be in 2010 June.

We thank the UK Science and Technology Facilities Council and the Italian Space Agency (ASI contract I/016/07/0 COFIS) for funding. This research has made use of the NASA/IPAC Extragalactic Database (NED), which is operated by the Jet Propulsion Laboratory, California Institute of Technology, under contract with the National Aeronautics and Space Administration.

[56] At www.h-atlas.org.

REFERENCES

Amblard, A., & Cooray, A. 2007, ApJ, 670, 903
Baldry, I., et al. 2010, MNRAS, 404, 86
Balogh, M., et al. 2004, MNRAS, 348, 1355
Bartelmann, M. 2001, A&A, 370, 754
Bartelmann, M., & White, S. 2002, A&A, 388, 732
Baugh, C., et al. 2005, MNRAS, 356, 1191
Beelen, A., et al. 2006, ApJ, 642, 694
Bendo, G., et al. 2003, AJ, 125, 2361
Bertoldi, F., et al. 2007, ApJS, 172, 132
Bregman, J. N., Snider, B. A., Grego, L., & Cox, C. V. 1998, ApJ, 499, 670
Browne, I. 2003, MNRAS, 341, 13
Cantalupo, C., Borrill, J., Jaffe, A., Kisner, T., & Stompor, R. 2010, ApJS, 187, 212
Cole, S., et al. 2000, MNRAS, 319, 168
Coleman, G. D., Wu, C.-C., & Weedman, D. W. 1980, ApJS, 43, 393
Colless, M., et al. 2001, MNRAS, 328, 1039
Coppin, K., et al. 2006, MNRAS, 372, 1621
Davies, J., & Burstein, D., ed. 1995, The Opacity of Spiral Disks
de Zotti, G., Ricci, R., Mesa, D., Silva, L., Mazzotta, P., Toffolatti, L., & Gonzalez-Nuevo, J. 2005, A&A, 431, 893
Devlin, M., et al. 2009, Nature, 458, 737
Devereux, N., & Young, J. S. 1990, ApJ, 359, 42
Dole, H., et al. 2006, A&A, 451, 417
Driver, S., et al. 2007, MNRAS, 379, 1022
Driver, S., et al. 2009, Astron. Geophys., 50, 12
Driver, S., Popescu, C., Tuffs, R., Graham, A., Liske, J., & Baldry, I. 2008, ApJ, 678, 101
Dunne, L., Eales, S. A., Edmunds, M., Ivison, R., Alexander, P., & Clements, D. L. 2000, MNRAS, 315, 115
Dunne, L., & Eales, S. 2001, MNRAS, 327, 697
Dunne, L., Eales, S., & Edmunds, M. 2003, MNRAS, 341, 589
Dwek, E., et al. 1998, ApJ, 508, 106
Dye, S., Smail, I., Swinbank, A., Ebeling, H., & Edge, A. 2007a, MNRAS, 379, 308
Dye, S., et al. 2007b, MNRAS, 375, 725
———. 2009, ApJ, 783, 285
Eales, S. A., et al. 1999, ApJ, 515, 518
———. 2009, ApJ, 707, 1779
Eddington, A. 1940, MNRAS, 100, 354
Fixsen, D. J., Dwek, E., Mather, J. C., Bennett, C. L., & Shafer, R. A. 1998, ApJ, 508, 123
Greve, T. R., Ivison, R. J., Bertoldi, F., Dunlop, J. S., Lutz, D., & Carilli, C. L. 2004, MNRAS, 354, 779
Greve, T. R., Pope, A., Scott, D., Ivison, R. J., Conselice, C. J., & Bertoldi, F. 2008, MNRAS, 389, 1489
Griffin, M., et al. 2007, Adv. Space Res., 40, 612
Frayer, D. T., et al. 2006, AJ, 131, 250
Frayer, D. T., et al. 2006, ApJ, 647, L9
Haas, M., et al. 2003, A&A, 402, 87
Heavens, A., Panter, B., Jimenez, R., & Dunlop, J. 2004, Nature, 428, 625
Helou, G., Rowan-Robinson, M., & Helou, G. 1986, ApJ, 298, L7
Holmberg, E. 1958, Medd. Lund. Astron. Obs. Ser., 2, 6
Hughes, D., et al. 1998, Nature, 394, 241
Ibar, E., et al. 2009, MNRAS, 386, 953
Jester, S., et al. 2005, AJ, 130, 873
Johnstone, S., et al. 2007, PASA, 24, 174
Kashlinsky, A., & Atrio-Barandela, F. 2000, AJ, 536, L67
Kauffmann, G., et al. 2003a, MNRAS, 341, 33
Kauffmann, G., et al. 2003b, MNRAS, 341, 54
Kauffmann, G., et al. 2004, MNRAS, 353, 713
Keller, S., Schmidt, B. P., & Bessell, M. S. 2007, Proceedings of the ESO Calibration Workshop, preprint (astroph 0704.1339)
Lagache, G., Dole, H., & Puget, J.-L. 2003, MNRAS, 338, 555
Lagache, G., et al. 2004, ApJS, 154, 112
Lagache, G., et al. 2007, ApJ, 665, L 89
Lewis, I., et al. 2002, MNRAS, 334, 673
Loveday, J., et al. 2004, MNRAS, 347, 601
Magorrian, J., et al. 1998, AJ, 115, 2285
Maddox, S., Efstathiou, G., & Sutherland, W. 1990, MNRAS, 246, 433
Mivilles-Deschenes, M.-A., et al. 2007, A&A, 459, 595
Negrello, M., et al. 2007, MNRAS, 377, 1557
Obric, M., et al. 2006, MNRAS, 370, 1677
Oliver, S., et al. 2010, in preparation
Perera, T. A., et al. 2008, MNRAS, 391, 1227

Poglitsch, A., et al. 2006, Proc. SPIE, 6265, 8
Priddey, R., et al. 2003, MNRAS, 339, 1183
Rowan-Robinson, M. 2001, ApJ, 549, 745
Saunders, W., et al. 1990, MNRAS, 242, 318
Scott, S., et al. 2002, MNRAS, 331, 817
Scott, K. S., et al. 2008, MNRAS, 385, 2225
Serjeant, S., & Hatziminaoglou, E. 2009, MNRAS, 397, 265
Smail, I., Ivison, R., & Blain, A. 1997, ApJ, 490, 5
Strauss, M., et al. 2002, AJ, 124, 1810
Takeuchi, T. T., Ishii, T. T., Dole, H., Dennefeld, M., Lagache, G., & Puget, J.-L. 2006, A&A, 448, 525
Van Kampen, E., et al. 2005, MNRAS, 359, 469
Vlahakis, C., Dunne, L., & Eales, S. 2005, MNRAS, 364, 1253
Vlahakis, C., Dunne, L., & Eales, S. 2007, MNRAS, 379, 1042
Warren, S., et al. 2007, preprint (astroph 0703037)
Waskett, T. J., Sibthorpe, B., Griffin, M. J., & Chanial, P. F. 2007, MNRAS, 381, 1583
Waskett, T. J., Sibthorpe, B., & Griffin, M. J. 2006, Studying Galaxy Evolution with Spitzer and Herschel, preprint (astro-ph 0609783)
York, D. G., et al. 2000, AJ, 120, 1579
Zemcov, M., et al. 2007, MNRAS, 376, 1073